Molecular Pharmacology Fast Forward. Published on November 29, 2012 as DOI: 10.1124/mol.112.081372
Molecular Pharmacology Fast Forward. Published on November 29, 2012 as doi:10.1124/mol.112.081372
This article has not been copyedited and formatted. The final version may differ from this version.

Bisphenol A inhibits voltage-activated Ca^{2+} channels *in vitro*: mechanisms and structural requirements

André Deutschmann, Michael Hans, Rainer Meyer, Hanns Häberlein

and Dieter Swandulla

Institute of Physiology II (A.D., M.H., R.M., D.S.); Institute for Biochemistry and Molecular Biology (H.H.), University of Bonn, Nussallee 11, Bonn 53115, Germany

Downloaded from molpharm.aspetjournals.org at ASPET Journals on April 17, 2024

Copyright 2012 by the American Society for Pharmacology and Experimental Therapeutics.

Molecular Pharmacology Fast Forward. Published on November 29, 2012 as DOI: 10.1124/mol.112.081372
This article has not been copyedited and formatted. The final version may differ from this version.

Running title: Bisphenol A inhibits voltage-activated Ca^{2+} channels

Correspondence to D. Swandulla, Institute of Physiology II, University of Bonn, Nussallee 11, 53115 Bonn. Telephone: +49 (0228)-7360101. Fax: 49 (0228)-7360119. E-mail: dieter.swandulla@ukb.uni-bonn.de

Number of text pages: 30

Number of tables: 2

Number of figures: 8

Number of references: 45

Number of words in the Abstract: 245

Number of words in the Introduction: 592

Number of words in the Discussion: 938

Abbreviations: BPA, bisphenol A; DRG, dorsal root ganglion; HEK, human embryonic kidney; LVA, low voltage-activated; HVA, high voltage-activated; PDI, protein disulfide isomerase; TEA, tetraethylammonium; EGTA, ethylene glycol-bis(2-aminoethylether)-N,N,N′,N′-tetraacetic acid; HEPES, 4-(2-hydroxyethyl)-1-piperazineethanesulfonic acid; 4´-CP, 4-(1-methyl-1-phenylethyl)-phenol; 2,2´-DPP, 1,1'-(1-methylethylidene)bis-benzene; BPAF, 4,4'-(1,1,1,3,3,3-hexafluoro-2,2-propanediyl)diphenol; BPE, 4,4'-ethylidene-diphenol; BPAB, 4,4'-(2,2-butanediyl)diphenol; BPF, 4,4'- methylenebis-phenol; 4,4´-HBP, 4,4'-dihydroxybenzophenone; BPS, 4,4'-sulfonyldiphenol; Biphenol, 4'-diol-1,1-biphenyl; TBBA, 4,4'-(1-methylethylidene)bis-2,6-dibromo-phenol; TMBPA, 4,4'-isopropylidenebis(2,6-dimethylphenol); 4´-TBP, 4-tert-butyl-phenol; 4´-TAP, 4-(1,1-dimethylpropyl)-phenol; BPM, 4,4'-((p-phenylene)diisopropylidene)diphenol; BPP, 4,4'-((p-phenylene)diisopropylidene)diphenol.

Downloaded from molpharm.aspetjournals.org at ASPET Journals on April 17, 2024

Molecular Pharmacology Fast Forward. Published on November 29, 2012 as DOI: 10.1124/mol.112.081372
This article has not been copyedited and formatted. The final version may differ from this version.

Abstract

Bisphenol A (BPA), a high volume production chemical compound attracts growing attention as health relevant xenobiotic in humans. It can directly bind to hormone receptors, enzymes and ion channels to become biologically active. In this study we show that BPA acts as a potent blocker of voltage-activated Ca^{2+} channels. We determined the mechanisms of block and the structural elements of BPA essential for its action. Macroscopic Ba^{2+}/ Ca^{2+} currents through native L-, N-, P/Q-, T-type Ca^{2+} channels in rat endocrine GH_3 cells, mouse DRG neurons or cardiac myocytes and recombinant human R-type Ca^{2+} channels expressed in HEK293 cells were rapidly and reversibly inhibited by BPA with similar potency (EC_{50} values: 26 to 35 µM). Pharmacological and biophysical analysis of R-type Ca^{2+} channels revealed that BPA interacts with the extracellular part of the channel protein. Its action does not require intracellular signaling pathways, is neither voltage- nor use-dependent and does not affect channel gating. This indicates that BPA interacts with the channel in its resting state by directly binding to an external site outside the pore forming region. Structure-effect analyses of various phenolic and bisphenolic compounds revealed that (i) a double-alkylated (R-$C(CH_3)_2$-R, R-$C(CH_3)(CH_2CH_3)$-R), or double-trifluoromethylated sp^3 hybridized carbon atom between the two aromatic rings and (ii) the two aromatic moieties in angulated orientation are optimal for BPA´s effectiveness. Since BPA highly pollutes the environment and is incorporated into the human organism our data may provide a basis for future studies relevant for human health and development.

Downloaded from molpharm.aspetjournals.org at ASPET Journals on April 17, 2024

Molecular Pharmacology Fast Forward. Published on November 29, 2012 as DOI: 10.1124/mol.112.081372
This article has not been copyedited and formatted. The final version may differ from this version.

Introduction

Bisphenol A (BPA) is a chemical which is extensively used (> 3.8 million tons/year worldwide) to produce polycarbonate plastic and epoxy resins. Both synthetics are manufactured into highly diverse mass products such as, optical media (CD, DVD), protective coatings inside metal food containers, baby bottles, thermal paper, composites and sealants in dentistry and medical tubing (for review see Dekant and Völkel, 2007; Vandenberg et al., 2007). BPA is an environmental pollutant which is incorporated into living organisms (for review see von Goetz et al., 2010). Common routes of BPA exposure in humans are oral intake, respiration and dermal absorption (Biedermann et al., 2010; Braunrath, 2005; Loganathan and Kannan, 2011). Detectable levels of BPA were found in over 90 % of people living in industrialized countries most likely due to chronic exposure (Calafat et al., 2005; Calafat et al., 2008; see also He et al., 2009). BPA´s adverse effects on human health and the ecosphere are being increasingly recognized (for review see Chapin et al., 2008).

Numerous studies have shown that BPA influences a wide range of physiological functions (for review see Rubin, 2011). It is very well documented that BPA and various related compounds bind to hormone receptors and influence multiple endocrine pathways (Matsushima et al., 2008; Okada et al., 2008; Riu et al., 2011; Soriano et al., 2012; Swedenborg et al., 2009). Beyond this, recent studies provide evidence that BPA can directly interact with biologically active proteins such as enzymes and ion channels (Asano et al., 2010; Hashimoto et al., 2012; Hiroi et al., 2006; O'Reilly et al., 2012; Pandey and Deshpande, 2012). Protein disulfide isomerase (PDI) has been isolated as a binding protein of BPA in the rat brain. BPA binds to different domains of PDI with K_D´s in the range of 10^{-6} to 10^{-3} molar (Hashimoto et al., 2012). A rapid and reversible increase of large conductance Ca^{2+}/voltage-sensitive K^+ (Maxi-K) channel activity by BPA (10 – 100 µM) has been shown

Downloaded from molpharm.aspetjournals.org at ASPET Journals on April 17, 2024

Molecular Pharmacology Fast Forward. Published on November 29, 2012 as DOI: 10.1124/mol.112.081372
This article has not been copyedited and formatted. The final version may differ from this version.

in human and canine coronary smooth muscle cells as well as in AD-293-cells expressing the recombinant form of the channel (Asano et al., 2010). Furthermore inhibitory effects of BPA in the micromolar range have been reported for mouse neuronal (Wang et al., 2011) and human cardiac Na^+ channels (O'Reilly et al., 2012). In the latter case it has been shown that BPA directly binds to the channel protein at the local anesthetic receptor site.

In the present study we have characterized the interaction of BPA and several of its related compounds with voltage-activated Ca^{2+} channels. This family of channels can be divided into subtypes which are expressed in different cells of the body (for review see Catterall et al., 2005). The different types of voltage-activated Ca^{2+} channels play key roles in various physiological and pathophysiological processes such as excitation-contraction coupling, synaptic transmission, hormone release, gene expression and cell death and differentiation (for review see Catterall, 2011).

We sought to elucidate the mechanisms underlying BPA´s interaction with voltage-activated Ca^{2+} channels expressed in GH_3 pituitary tumor cells, mouse DRG neurons, mouse cardiac myocytes and with voltage-activated recombinant human R-type Ca^{2+} channels stably expressed in HEK293 cells. The blocking mechanism of BPA was analyzed in detail in recombinant human R-type Ca^{2+} channels. We aimed at characterizing state dependence of the block and the site were BPA binds to the channel protein. Furthermore we intended to determine which structural features of the BPA molecule are basic for its ability to block Ca^{2+} channels. For that purpose we compared the degree of Ca^{2+} channel block induced by BPA related compounds to that of BPA.

Downloaded from molpharm.aspetjournals.org at ASPET Journals on April 17, 2024

Molecular Pharmacology Fast Forward. Published on November 29, 2012 as DOI: 10.1124/mol.112.081372
This article has not been copyedited and formatted. The final version may differ from this version.

Material and Methods

Cells and Cell Culture. Endocrine rat pituitary tumor cells (GH_3 line; DSMZ, Braunschweig, Germany) were grown on 100 * 20 mm culture dishes (Becton Labware, Frankling Lakes, USA) in Ham F10 Medium supplemented with 15 % horse serum, 2.5 % FCS, 1 % penicillin-streptomycin and 2 mM glutamine. 2-7 days before electrophysiological recordings cells were harvested with trypsin or accutase (PAA, Pasching, Austria) and plated on poly-L-lysine coated (Sigma, Taufkirchen, Germany) 6 mm glass coverslips in P.neural-Medium (P.Glia, Rheinbach, Germany) and maintained in humidified atmosphere (37°C). Cells were used for electrophysiological recordings within the following 48 h.

Dorsal root ganglion (DRG) neurons were excised from decapitated 4 to 14 day old male or female (ratio ~ 1:1) mice (C57BL/6) and incubated for 25 ± 5 min in extracellular solution consisting of (in mM): 124 NaCl, 2.5 KCl, 26 $NaHCO_3$, 1 NaH_2PO_4, 1.3 $MgSO_4$, 2 $CaCl_2$, 10 D-glucose, pH 7.35, gassed with carbogen (95 % O_2, 5 % CO_2) containing 0.04 % collagenase and 0.025 % trypsin type I (Roche, Mannheim, Germany) at 37°C. Digestion was stopped by resuspending the tissue in culture medium: DMEM/ F12 (1:1) (Invitrogen, Mannheim, Germany) supplemented with 10 % fetal bovine serum, penicillin (100 U/mL) and streptomycin (100 U/mL), and 2 mM L-glutamine (all Invitrogen). Tissue was triturated mechanically by vigorously shaking and centrifuged at 160×g for 5 min after filtration. Pellet was resuspended in culture medium and cells were plated on poly-L-lysine coated glass coverslips and kept in humidified atmosphere (37°C, 95 % air, 5 % CO_2). Cells of medium size were used for electrophysiological recordings within the following 12 h. All animal experiments were conducted in accordance with the guidelines of the Animal Care Committee of the University of Bonn.

Downloaded from molpharm.aspetjournals.org at ASPET Journals on April 17, 2024

Molecular Pharmacology Fast Forward. Published on November 29, 2012 as DOI: 10.1124/mol.112.081372
This article has not been copyedited and formatted. The final version may differ from this version.

Cardiac myocytes were isolated from male or female (ratio ~ 1:1) mice (C57BL/6) as described previously (Linz and Meyer, 2000). Briefly, hearts were removed and cardiopleged in cold Tyrode solution containing NaCl 135 mM, KCl 4 mM, $MgCl_2(H_2O)_6$ 1 mM, HEPES 2 mM, EGTA 2.6 mM, pH 7.4. The heart was rapidly attached to a Langendorff apparatus and perfused with the Tyrode solution described above (37°C) followed by a high potassium solution (NaCl 4 mM, KCl 10 mM, $MgCl_2$ 1 mM, $CaCl_2$ 0.2 mM, K-glutamate 130 mM). For digestion 200 U/mL trypsin type I (Sigma) and 0.4 mg/mL collagenase type II (Sigma) were added. The ventricles were cut down, chunked and allowed to settle in oxygenated Tyrode solution containing NaCl 135 mM, KCl 4 mM, $MgCl_2$ 1 mM, HEPES 2 mM, $CaCl_2$ 1.8 mM, BSA 1 mM and trypsin inhibitor 16.6 mg/L. The solution was filtered through a 125 µm nylon mesh centrifuged briefly and the pellet was resuspended in fresh Tyrode solution. Cells were plated on poly-L-lysine coated glass coverslips and recordings were performed 1-8 h after plating.

Human embryonic kidney (HEK) 293 cells stably expressing human α_{1E} and β_3 Ca^{2+} channel subunits (Sochivko et al., 2002) were maintained in DMEM supplemented with penicillin (100 U/mL), streptomycin (100 µg/mL) (Invitrogen, Darmstadt, Germany), and 10 % fetal bovine serum. Geneticin (0.5 mg/mL) and hygromycin (0.2 mg/mL) were used for selection of α_{1E} and β_3 subunit expression, respectively. Cells were plated on poly-L-lysine coated glass coverslips and used within 24-48 h after plating for recordings.

Electrophysiological recordings. Ca^{2+} and/or Ba^{2+} currents were recorded in the whole-cell configuration of the patch-clamp technique using an EPC9 patch-clamp amplifier and the PULSE software (HEKA Electronic, Lambrecht, Germany). Data were filtered and digitized at 3 and 10 kHz, respectively, and stored on hard disk. For recordings of tail currents the sampling rate was 100 kHz. In ventricular cardiac myocytes Ca_v 1.2 L-type Ca^{2+} channels

Downloaded from molpharm.aspetjournals.org at ASPET Journals on April 17, 2024

Molecular Pharmacology Fast Forward. Published on November 29, 2012 as DOI: 10.1124/mol.112.081372
This article has not been copyedited and formatted. The final version may differ from this version.

constitute the major pathway for HVA Ca^{2+} currents (Bers and Perez-Reyes, 1999). Ba^{2+} (2 mM) currents through these channels were elicited by voltage ramps (200 ms) from -50 mV to +70 mV. In mouse DRG neurons Ca^{2+} currents through T-type Ca^{2+} channels were evoked by depolarizations (100 ms) from -70 mV to -20 mV using Ca^{2+} (10 mM) as charge carrier. Currents through N-type Ca^{2+} channels were elicited by voltage ramps (100 ms) from -70 mV to +50 mV using Ba^{2+} (1 mM) as charge carrier. Currents were recorded in the presence of nifedipine (10 µM) and ω-Agatoxin-TK (0.2 µM) to eliminate contribution from L- and P/Q-type Ca^{2+} channels, respectively. The internal solution of the recording electrodes contained (in mM): cesium-aspartate 160, EGTA 10, Mg_2ATP 2, phosphocreatine 20, Na_2GTP 0.2, HEPES 20 (pH 7.3, 290-300 mOsmol/L). Filled electrodes had resistances between 1.5 and 4 MΩ. The extracellular solution contained in mM: tetraethylammonium (TEA)-Br 160, KCl 3, $BaCl_2$ or $CaCl_2$, $NaHCO_3$ 1, $MgCl_2$ 1, HEPES 10 Glucose 4 (pH 7.4, 300-310 mOsmol/L). The final concentrations of Ba^{2+} and Ca^{2+} are indicated in the text. All recordings were performed at room temperature (20-23°C).

The recording chamber was continuously perfused at a rate of 1 mL/min. The bath volume was exchanged every 20 s. Drugs were applied in external solution using a fast pressure-application system (DAD-VM Superfusion System, ALA Scientific Instruments, NY, USA). The tip of the application pipette (diameter 100 µm) was positioned within 100 µm off the cells and solution exchange was obtained within ~ 20 ms.

Drugs. Bisphenol A and the related compounds were purchased from Alfa Aesa (Karlsruhe, Germany) or Sigma-Aldrich (Taufkirchen, Germany). Stock solutions of the drugs were prepared in ethanol at a concentration of 200 mM and stored at room temperature. All toxins were obtained from Tocris Biosciences (Wiesbaden, Germany) and stock solutions were prepared in distilled water. Application solutions were freshly prepared from stock solution.

Downloaded from molpharm.aspetjournals.org at ASPET Journals on April 17, 2024

Molecular Pharmacology Fast Forward. Published on November 29, 2012 as DOI: 10.1124/mol.112.081372
This article has not been copyedited and formatted. The final version may differ from this version.

The highest final concentration of the solvent ethanol was 0.15 % which did not affect voltage-activated Ca^{2+} currents. All other chemicals were obtained from Sigma-Aldrich.

Data analysis and statistics. The analysis of the whole-cell recordings was carried out offline using PulseFit (HEKA, Germany) or IGOR software (Wavemetrics, Lake Oswego, OR, USA). Data fitting and statistical analysis were performed using PRISM 5.0 (GraphPad Software Inc., San Diego, CA, USA). EC_{50}s and Hill slopes were determined by fitting data points to a logistic function. Charge-voltage-relationships were fitted by an equation in the form $y = G_{max} * (V_{test} - V_{rev}) / (1 + \exp((V_{1/2} - V_{test}) / k))$ with G_{max} = maximum conductance, $V_{1/2}$ = half-maximal activation, V_{test} = test potential, V_{rev} = reversal potential and k = slope factor. Data for m_∞ and h_∞ were fitted to a Boltzmann function $Y = Min + (Max - Min) / (1 + \exp((V_{0.5} - V_{test}) / k))$. Time course for recovery from inactivation was fitted by a double exponential function. The data in the manuscript are presented as mean ± standard error unless stated otherwise. Statistical analysis was performed using Students *t*-test or one way analysis of variance (ANOVA) and Tukey´s post-test. Differences with p-value < 0.05 were regarded as significant.

Downloaded from molpharm.aspetjournals.org at ASPET Journals on April 17, 2024

Molecular Pharmacology Fast Forward. Published on November 29, 2012 as DOI: 10.1124/mol.112.081372
This article has not been copyedited and formatted. The final version may differ from this version.

Results

Inhibition of high voltage-activated (HVA) Ca^{2+} channels by BPA in GH_3 cells. GH_3 cells used in our experiments express essentially HVA Ca^{2+} channels. BPA was applied extracellularly to single cells at micromolar concentrations using a fast application system (see Materials and Methods). Fig. 1A shows the effect of BPA on Ba^{2+} currents (5 mM) elicited by depolarizing voltage steps (50 ms) to 0 mV at 0.1 Hz for three different concentrations. Each concentration (starting with 10 µM) was applied for 40 s during which maximal inhibition was achieved. The current inhibition was almost fully reversible and currents recovered completely within about 1 min upon washout of BPA. Similar results were obtained with Ca^{2+} (10 mM) as charge carrier. Note, that internal perfusion with BPA even at high concentrations (100 µM) was ineffective (data not shown). Fig. 1B illustrates the time course of Ca^{2+} channel block by 100 µM BPA and of its washout when brief depolarizing steps (15 ms) to 0 mV were applied at 1 Hz. The finding that the amount of block by BPA did not vary with different stimulation frequencies (0.1 and 1 Hz) implies that the block is not use dependent (for a more detailed analysis see R-type Ca^{2+} channels).

In further experiments the effect of BPA (70 µM) was studied at different depolarizing voltages. The charge transferred by individual Ba^{2+} currents was determined from the area under the current curves. Fig. 1C shows the charge-voltage relationship (C/V) obtained in the presence and absence of BPA. While charge transfer was significantly reduced there was no significant shift in the C/V curve in the presence of BPA. The mean value of the block at different membrane potentials was calculated from corresponding data points and plotted against voltage (fractional block, see inset). The degree of block did not vary significantly within the voltage range tested ($p = 0.92$; $n = 3$).

Downloaded from molpharm.aspetjournals.org at ASPET Journals on April 17, 2024

Molecular Pharmacology Fast Forward. Published on November 29, 2012 as DOI: 10.1124/mol.112.081372
This article has not been copyedited and formatted. The final version may differ from this version.

To analyze the blocking action of BPA in more detail total currents were pharmacologically dissected using nifedepine and/or ω-conotoxins. As illustrated in Fig. 1 D1 the application of ω-conotoxin GVIA (1.5 µM) was ineffective, indicating that N-type channels did not contribute to the total current. Application of nifedepine (10 µM) which blocks L-type Ca^{2+} channels resulted in a 52 ± 3.9 % (n = 6) reduction of the total current. Block of P/Q-type Ca^{2+} channels by ω-conotoxin MVIIC (1.5 µM) reduced the total current by 30 ± 0.9 % (n = 7). A small current fraction (probably R-type) of 17 ± 2.0 % (n = 3) of the total current was resistant to both nifedepine and ω–conotoxin MVIIC. Fig. 1 D2 illustrates the contribution of the different HVA Ca^{2+} channel types to the total current.

In the presence of BPA (70 µM) the total Ba^{2+} current was inhibited by 74.2 ± 2.6 % (n = 7; Fig. 1 E1). Fig. 1 E2 shows that inhibition of the current components remaining after nifedepine and/or ω-conotoxin MVIIC application did not significantly differ from inhibition of the total current by BPA ($p > 0.7$ between the four columns). These findings indicate that BPA does not discriminate between the different HVA Ca^{2+} channel types and blocks L-, P/Q-, and probably R-type Ca^{2+} channels to the same extend.

Fig. 1F illustrates the concentration-effect relationship for total Ba^{2+} currents and currents in the presence of nifedepine. The potency of BPA to inhibit currents is similar for both curves (see Table 1). This supports our findings that BPA does not distinguish between the different HVA channel types.

Inhibition of high and low voltage-activated (HVA, LVA) Ca^{2+} channels by BPA in DRG neurons. In DRG neurons N-type Ca^{2+} channels are predominant (Fig. 2A2) as indicated by the finding that 78 ± 0.6 % (n=3) of the total Ba^{2+} currents were blocked by the

Downloaded from molpharm.aspetjournals.org at ASPET Journals on April 17, 2024

Molecular Pharmacology Fast Forward. Published on November 29, 2012 as DOI: 10.1124/mol.112.081372
This article has not been copyedited and formatted. The final version may differ from this version.

application of ω-conotoxin GVIA (500 nM) (Fig. 2A1). Application of nifedipine (10 μM) reduced the current by 15 ± 1.7 %. Application of agatoxin TK (200 nM), a P/Q-type Ca^{2+} channel blocker, was ineffective. A small current fraction (~ 6 %) was resistant to the blockers applied and was presumably through R-type Ca^{2+} channels (Fig. 2A2). Dose dependent inhibition of N-(+R-) type channels by BPA was studied in the presence of nifedipine and agatoxin TK (Fig. 2B). The EC_{50} of 35 ± 1.3 μM was comparable to the EC_{50} values obtained for other HVA Ca^{2+} channel types in GH_3 cells. In DRG neurons the effect of BPA was also investigated on low voltage-activated (T-type) Ca^{2+} channels. BPA reduced also this type of Ca^{2+} channels with a potency comparable to that obtained for HVA Ca^{2+} channel types (Fig. 2C; Table 1).

Inhibition of L-type Ca^{2+} channels by BPA in cardiac myocytes. In ventricular cardiac myocytes HVA Ca^{2+} currents are through Ca_v 1.2 L-type Ca^{2+} channels (Bers and Perez-Reyes, 1999). BPA inhibited these Ca^{2+} channels in a concentration dependent manner with an EC_{50} of 35 ± 1.3 μM (Fig. 2D). As in endocrine and neuronal cells the time course of block and of its washout was fast and occurred within seconds. Together these findings suggest that BPA inhibits the different classes of Ca^{2+} channel found in different tissues with similar potency (for summary see Table 1).

Biophysical and pharmacological characterization of BPA´s action on human R-type Ca^{2+}channels expressed in HEK293 cells. A detailed analysis of the blocking mechanisms of BPA was performed on human R-type Ca^{2+} channels in HEK293 cells stably expressing α_{1E} and β_3 Ca^{2+} channel subunits. Fig. 3A shows a family of Ba^{2+} (15 mM) currents elicited by depolarizing steps (100 ms) to voltages between -10 and +40 mV. BPA (35 μM; middle

Downloaded from molpharm.aspetjournals.org at ASPET Journals on April 17, 2024

Molecular Pharmacology Fast Forward. Published on November 29, 2012 as DOI: 10.1124/mol.112.081372
This article has not been copyedited and formatted. The final version may differ from this version.

panel) reversibly inhibited currents and nearly full recovery from current inhibition was observed within 2 min upon washout (Fig. 3A right panel). Small reductions in current amplitudes after washout were most likely due to current rundown during internal perfusion. In some cells full recovery could be obtained. To test for use dependence of the block depolarizing steps (15 ms) to 0 mV were applied at 0.1, 1 and 10 Hz. The amount of block obtained by BPA (35 μM) at each frequency did not vary significantly ($p = 0.88$; data not shown; see also Fig. 1A, B). This was also the case when the frequency was changed to 10 Hz after block had reached its equilibrium at 0.1 or 1 Hz.

Fig. 3B illustrates the charge transferred by Ba^{2+} ions through R-type Ca^{2+} channels at different depolarizing voltages for control and in the presence of 35 μM BPA (C/V relationship). Inhibition of Ba^{2+} currents through R-type Ca^{2} channel by BPA was concentration dependent and occurred with an EC_{50} of 26 ± 1 μM (Fig. 3C).

To test whether binding of BPA is state dependent holding potential was shifted from -70 mV to -100 mV where almost all of the channels are in the resting state (Fig. 4A). As we did not observe any significant change in potency (Fig. 3C; EC_{50} 32 ± 1 μM; $p = 0.66$), this finding strongly suggests that BPA binds to the channel in its resting state.

As illustrated in Fig. 3A current activation and inactivation kinetics were hardly affected by BPA. In further experiments we determined steady state activation and inactivation under control conditions and in the presence of 35 μM BPA (Fig. 4A) and found that neither the steady state activation nor the inactivation curves were significantly affected by BPA. Taken together these findings provide additional evidence that BPA binds to and stabilizes the resting state of the channel. Further support comes from the observation that neither recovery from inactivation (Fig. 4B; $p = 0.824$) nor deactivation kinetics (Fig. 4C; $p = 0.73$) were significantly changed by BPA.

Downloaded from molpharm.aspetjournals.org at ASPET Journals on April 17, 2024

Molecular Pharmacology Fast Forward. Published on November 29, 2012 as DOI: 10.1124/mol.112.081372
This article has not been copyedited and formatted. The final version may differ from this version.

To exert its action BPA has to be present for a certain time period (pre-application time) before current activation. When pre-applied for 100 ms BPA (70 µM) started to become effective and approached its maximal inhibitory effect after 10 s of pre-application (Fig. 5A). When block was brought to equilibrium by prolonged pre-application (3 min) of BPA (35 µM) before a long-lasting depolarizing step (1 s) was applied we observed only a reduction in current amplitude and no change in the rate of current decay (Fig. 5C, D). These findings demonstrate that BPA is not blocking open channels. Further support for these results came from the observation that BPA did neither affect current amplitude nor current kinetics when applied during depolarizing pulses with channels in the open state (Fig. 5B). Even concentrations as high as 300 µM did not produce any current inhibition.

To test for a possible involvement of intracellular signaling pathways in BPA´s action modulators of G-proteins and protein kinase A and C were applied (Fig. 6). Irreversible activation or inhibition of G proteins by adding GTP-γ-S (20 µM) or GDP-β-S (1 mM) to the internal perfusion solution, respectively, had no significant effect on the blocking action of BPA. Neither was BPA´s action affected by the inhibition of protein kinases A and C by H-89 (10 µM) and GÖ-6983 (10 µM), respectively. These modulators were applied extracellularly for up to 10 min. It is noteworthy that GÖ-6983 itself inhibited Ca^{2+} channels to about 77.6 ± 1.8 % (n = 3) after 4-5 min. Similar effects of GÖ-6983 have been previously described for L-type Ca^{2+} channels (Welling et al., 2005). BPA was always applied after the inhibitory effect of GÖ-6983 had reached its maximum.

Several reports have suggested or demonstrated that hormones are able to modulate Ca^{2+} channels by direct interaction (for review see Boonyaratanakornkit and Edwards, 2007). In particular 17β-estradiol (E_2) has been shown to rapidly and reversibly reduce cardiovascular L-type Ca^{2+} channels at micromolar concentrations (Jiang et al., 1992; Meyer et al., 1998; Nakajima et al., 1995). Since we found that BPA inhibited L-type Ca^{2+} channels in

Downloaded from molpharm.aspetjournals.org at ASPET Journals on April 17, 2024

Molecular Pharmacology Fast Forward. Published on November 29, 2012 as DOI: 10.1124/mol.112.081372
This article has not been copyedited and formatted. The final version may differ from this version.

cardiomyocytes (Fig. 2D) we were wondering if it shares a common binding site on Ca^{2+} channels with E_2. Indeed E_2 (100 µM) also reduced R-type Ca^{2+} channels rapidly and reversibly by 40.7 ± 2.3 % (Fig. 7A). At this concentration the E_2 mediated inhibition was near saturation (Fig. 7B), but was significantly smaller than that observed with BPA (more than 80 %) at the same concentration (Fig. 7A, B). Similar results were obtained with total currents in GH_3 cells (data not shown).

In case of a common binding site one would expect that under these conditions the combination of the two compounds is less effective than BPA alone. This, however, was not observed (Fig. 7A, B). On the contrary the combination of the two compounds was slightly but significantly more effective (BPA: 81.5 ± 1.3 %; n = 14; BPA + E_2: 85.6. ± 1.3 %; n = 12; $p < 0.05$).

Effect of BPA and related compounds on Ca^{2+} channels in GH_3 cells. To study the structure activity relationship of bisphenol A and related substances, compounds with (i) different bridging structures between the two phenolic rings (e.g. BPAF, BPF, 4,4´-HBP), (ii) different aromatic substitution patterns (4´-CP, 2,2´-DPP, TMBPA), and (iii) different sterically demanding structure moieties (4´-TBP, 4´-TAP, BPM, BPP) were investigated in GH_3 cells (Fig. 8). Table 2 summarizes the effect of the various phenolic and bisphenolic compounds on HVA Ba^{2+} currents in GH_3 cells in relation to BPA.

TBBA one of the most abundantly produced halogenated flame retardants effectively inhibited Ba^{2+} currents at 100 µM concentration. As shown in Fig. 8A TBBA was slightly but significantly less effective in blocking Ca^{2+} channels than BPA (Table 2). In contrast, BPS another high production monomer had no significant effect at this high concentration (Table 2).

Downloaded from molpharm.aspetjournals.org at ASPET Journals on April 17, 2024

Molecular Pharmacology Fast Forward. Published on November 29, 2012 as DOI: 10.1124/mol.112.081372
This article has not been copyedited and formatted. The final version may differ from this version.

Comparing the effect of BPA, 4´-CP, 2,2´-DPP, TBBA, and TMBPA, the aromatic substitution pattern strongly influences the ability to inhibit Ca^{2+} channels. The chemical structure of BPA is composed of two methyl groups and two phenol moieties on the central sp^3-hybridized carbon atom. 4´-CP which lacks one phenol-hydroxyl group was about half as active as BPA. 2,2´-DPP lacking both of the phenol-hydroxyl groups was ineffective (< 20 %). Furthermore, four aromatic methyl groups at meta-position (TMBPA) decrease the activity, whereas TBBA with four bromines as substituents was almost as active as BPA. Obviously, an aromatic substituent like bromine with a positive mesomeric effect and a predominant negative inductive effect supports the ability of meta-substituted compound to inhibit Ca^{2+} channels by reducing the electron density of π-systems.

In addition, the double methylated sp^3-hybridized carbon atom, present in BPA and TBBA, which bridges the two phenol rings is optimal for the ability of the compounds to inhibit Ca^{2+} channels. In fact, successive removal of the methyl groups revealed less effective bisphenols (BPE, BPF). Remarkably, BPAF where the methyl groups are replaced with trifluoromethyl moieties was twice as potent as BPA (EC_{50} = 13 ± 1.15 µM, data not shown). BPAB which has a bulky bridging structure (R-C(CH_3)(CH_2CH_3)-R) was almost equally effective compared to BPA. Furthermore, sp^2-hybridization of this carbon atom or introduction of different bridging structures led to bisphenols which were ineffective (4´4- HBP, BPS). It is interesting to note, that biphenol did not show any activity which again confirms that a sp^3-hybridized carbon atom bridging the aromatic rings is essential for the blocking effect on Ca^{2+} channels.

Apparently, two aromatic ring moieties in angulated orientation are required for Ca^{2+} channel block. The blocking activity of compounds lacking one of the aromatic rings (4´-TBP; 4´-TAP) was much less pronounced than that of BPA (Fig. 8B; Table 2). Finally, the ability to

Downloaded from molpharm.aspetjournals.org at ASPET Journals on April 17, 2024

Molecular Pharmacology Fast Forward. Published on November 29, 2012 as DOI: 10.1124/mol.112.081372
This article has not been copyedited and formatted. The final version may differ from this version.

inhibit Ca^{2+} channels by sterically demanding bisphenols like BPM strongly depends on the spatial orientation of all aromatic rings. In BPM which blocked voltage-activated Ca^{2+} channels by ~ 70 % these rings are arranged in line. In case the molecule is angulated as in BPP where one of the aromatic rings is rotated almost through 90° to form a right-angled structure inhibition of voltage-activated Ca^{2+} channels was negligible.

Downloaded from molpharm.aspetjournals.org at ASPET Journals on April 17, 2024

Molecular Pharmacology Fast Forward. Published on November 29, 2012 as DOI: 10.1124/mol.112.081372
This article has not been copyedited and formatted. The final version may differ from this version.

Discussion

In this study we present evidence that BPA interacts with voltage-activated Ca^{2+} channels as inhibitory ligand. BPA´s efficacy as inhibitor is comparable to that of polyvalent cations such as cadmium, cobalt and manganese (Carbone and Swandulla, 1989). Pharmacological experiments with specific organic blockers (nifedepine and ω-conotoxins) for the different Ca^{2+} channel types showed that BPA affects all subtypes studied here (L-, N-, P/Q-, R-, T-type) to the same extent. Detailed analysis of biophysical properties on human R-type channels revealed that channel kinetics (activation, inactivation and deactivation) and steady state characteristics (activation and inactivation) were not significantly altered by BPA.

In summary, our biophysical and pharmacological analysis strongly suggests that BPA exerts its action by binding to the channels in their resting state. This is supported by the findings that (i) the amount of block is independent of the frequency and duration of current activation, (ii) the current kinetics are not altered, (iii) there is no shift in the steady state inactivation curve. Furthermore our findings suggest that the binding site is located at the extracellular part of the pore forming subunit. BPA as a highly lipophilic substance might reach a binding site at the transmembranal part of the channel protein. However, when applied intracellularly BPA was ineffective.

Direct evidence that BPA interacts with a specific binding site comes from the analysis of structurally related phenol and bisphenol derivatives. In order to be effective the molecules have to meet certain structural requirements. From the binding motive of a double-methylated or double-trifluoromethylated sp^3-hybridized carbon atom flanked by two phenol moieties in angulated orientation one can strongly assume a specific binding site at the various Ca^{2+} channels which interacts with effective compounds. The ability of BPA and related

Downloaded from molpharm.aspetjournals.org at ASPET Journals on April 17, 2024

Molecular Pharmacology Fast Forward. Published on November 29, 2012 as DOI: 10.1124/mol.112.081372
This article has not been copyedited and formatted. The final version may differ from this version.

compounds to specifically interact with proteins has already been demonstrated for certain hormone receptors (Matsushima et al., 2007). Similar findings were described for BPA estrogen-related receptor-γ (ERR-γ) interactions. Whereas BPA (IC_{50} = 9.78 ± 0.87 nM) showed a high binding affinity to ERR-γ BPF was approx. (IC_{50} = 131 ± 17.9 nM) 16-fold less potent, which clearly demonstrated the importance of the double-methylated central carbon atom for ERR-γ interactions. (Matsushima et al., 2008; Okada et al., 2008). In BPAF the two methyl groups are replaced by two electron-rich trifluoromethyl moieties, which reduced the binding affinity to the ERR-γ considerably by a factor of 35. In contrast, the inhibitory effect on Ca^{2+} channels was more pronounced with BPAF compared to BPA. Furthermore, 2,2´-DPP lacking both of the phenol-hydroxyl groups did not show any ERR-γ binding, compared to 4´-CP, which was as active as BPA. Although there are some matches in the compound´s activity profiles for ERR-γ and Ca^{2+} channels we do not assume that the two binding sites for BPA possess major structural similarities on the two proteins.

Since BPA and several of its related compounds are environmental pollutants which can be incorporated into the human organism exposure to these chemicals may cause serious health problems. Urinary levels of BPA have recently been associated with chronic diseases, including heart disease, diabetes as well as neurobehavioral changes in toddlers (Lang et al., 2011; Melzer et al., 2010; Sathyanarayana et al., 2011).

The Environmental Protection Agency considers a save level of exposure to be 50 µg/kg of body weight/day (U.S.EPA, 2010). Recent experiments with primates, however, indicate that human exposure may be much higher than previously assumed (Taylor et al., 2010). Under certain conditions exposure to BPA may exceed putative save levels. This could be the case in manufacturing facilities. Indeed recent studies have shown that workers in epoxy resin factories can have approximately 1000 times higher urinary BPA concentrations compared to

Downloaded from molpharm.aspetjournals.org at ASPET Journals on April 17, 2024

Molecular Pharmacology Fast Forward. Published on November 29, 2012 as DOI: 10.1124/mol.112.081372
This article has not been copyedited and formatted. The final version may differ from this version.

control groups (He et al., 2009; Melzer et al., 2010; Wang et al., 2012). The highest levels measured were almost up to 10 µM (Wang et al., 2012) which is within the effective concentration range of Ca^{2+} channels block by BPA. High exposure to BPA has also been reported for patients particularly premature infants undergoing intensive medical care treatment (Calafat et al., 2009).

In general the incorporation of the lipid soluble compound BPA in certain body compartments is not very well studied and it is conceivable that BPA could accumulate to micromolar concentrations in the human body (see above). This may apply also to highly lipophilic, halogenated BPA derivatives such as tetrabromobisphenol A (TBBA) one of today´s most abundantly used brominated flame retardants. Indeed, it has been shown that in mice which have been fed with 100 µg TBBA/kg body weight TBBA accumulates overproportional in the striatum compared to other brain regions (Nakajima et al., 2009).

The toxicity of BPA has been evaluated with respect to development, reproduction and cancer (see e.g. Fernandez et al., 2012; Xu et al., 2010). In this context a recent FDA update points to “some concern about the potential effect (of BPA) on the brain, behavior and prostate gland in fetuses, infants and young children” (for review see Wolstenholme et al., 2011). The BPA concentration administered in toxicological studies is expected to result in micromolar concentrations in different compartments of the body and should critically depend on BPA metabolism. Exact values in humans, however, are currently not available.

Given the fact that BPA and its related compounds are ubiquitously contaminating our environment we expect that further studies will surface that medical diseases such as cardiovascular, respiratory, and metabolically caused disorders can at least partly be attributed to the effect of BPA on voltage-activated Ca^{2+} channels. Our findings that certain BPA related compounds are less or even non effective on voltage-activated Ca^{2+} channels

Downloaded from molpharm.aspetjournals.org at ASPET Journals on April 17, 2024

Molecular Pharmacology Fast Forward. Published on November 29, 2012 as DOI: 10.1124/mol.112.081372
This article has not been copyedited and formatted. The final version may differ from this version.

may provide a key in finding molecules which could substitute for BPA in large scale plastic production.

Downloaded from molpharm.aspetjournals.org at ASPET Journals on April 17, 2024

Molecular Pharmacology Fast Forward. Published on November 29, 2012 as DOI: 10.1124/mol.112.081372
This article has not been copyedited and formatted. The final version may differ from this version.

Acknowledgements: We are grateful to T. Schneider for providing the α_{1E} Ca^{2+} channel expressing cell line and we thank M. Zweyer and H. Bock for excellent technical assistance.

Authorship Contributions

Participated in research design: Swandulla, Hans, and Meyer
Conducted experiments: Deutschmann, Swandulla, and Hans
Performed data analysis: Deutschmann, Hans, Swandulla, Häberlein, and Meyer
Wrote or contributed to the writing of the manuscript: Swandulla, Hans, Häberlein, Meyer, and Deutschmann

Downloaded from molpharm.aspetjournals.org at ASPET Journals on April 17, 2024

Molecular Pharmacology Fast Forward. Published on November 29, 2012 as DOI: 10.1124/mol.112.081372
This article has not been copyedited and formatted. The final version may differ from this version.

References

Asano S, Tune JD and Dick GM (2010) Bisphenol A activates Maxi-K (KCa1.1) channels in coronary smooth muscle. *Br J Pharmacol* **160**: 160-170.

Bers DM and Perez-Reyes E (1999) Ca channels in cardiac myocytes: structure and function in Ca influx and intracellular Ca release. *Cardiovasc Res* **42**: 339-360.

Biedermann S, Tschudin P and Grob K (2010) Transfer of bisphenol A from thermal printer paper to the skin. *Anal Bioanal Chem* **398**: 571-576.

Boonyaratanakornkit V and Edwards DP (2007) Receptor mechanisms mediating non-genomic actions of sex steroids. *Semin Reprod Med* **25**: 139-153.

Braunrath (2005) Determination of Bisphenol A in canned foods by immunoaffinity chromatography, HPLC, and fluorescence detecton. *J Agric Food Chem* **53**: 8911-8917.

Calafat AM, Kuklenyik Z, Reidy JA, Caudill SP, Ekong J and Needham LL (2005) Urinary concentrations of bisphenol A and 4-nonylphenol in a human reference population. *Environ Health Perspect* **113**: 391-395.

Calafat AM, Weuve J, Ye X, Jia LT, Hu H, Ringer S, Huttner K and Hauser R (2009) Exposure to bisphenol A and other phenols in neonatal intensive care unit premature infants. *Environ Health Perspect* **117**: 639-644.

Calafat AM, Ye X, Wong LY, Reidy JA and Needham LL (2008) Exposure of the U.S. population to bisphenol A and 4-tertiary-octylphenol: 2003-2004. *Environ Health Perspect* **116**: 39-44.

Carbone E and Swandulla D (1989) Neuronal calcium channels: kinetics, blockade and modulation. *Prog Biophys Mol Biol* **54**: 31-58.

Catterall WA (2011) Voltage-gated calcium channels. *Cold Spring Harb Perspect Biol* **3**: a003947.

Catterall WA, Perez-Reyes E, Snutch TP and Striessnig J (2005) International Union of Pharmacology. XLVIII. Nomenclature and structure-function relationships of voltage-gated calcium channels. *Pharmacol Rev* **57**: 411-425.

Chapin RE, Adams J, Boekelheide K, Gray LE, Jr., Hayward SW, Lees PS, McIntyre BS, Portier KM, Schnorr TM, Selevan SG, Vandenbergh JG and Woskie SR (2008) NTP-CERHR expert panel report on the reproductive and developmental toxicity of bisphenol A. *Birth Defects Res B Dev Reprod Toxicol* **83**: 157-395.

Dekant W and Völkel W (2007) Human exposure to bisphenol A by biomonitoring: methods, results and assessment of environmental exposures. *Toxicol Appl Pharmacol* **228**: 114-134.

Fernandez SV, Huang Y, Snider KE, Zhou Y, Pogash TJ and Russo J (2012) Expression and DNA methylation changes in human breast epithelial cells after bisphenol A exposure. *Int J Oncol* **41**: 369-377.

Hashimoto S, Shiomoto K, Okada K and Imaoka S (2012) The binding site of bisphenol A to protein disulphide isomerase. *J Biochem* **151**: 35-45.

He Y, Miao M, Herrinton LJ, Wu C, Yuan W, Zhou Z and Li D-K (2009) Bisphenol A levels in blood and urine in a chinese population and the personal factors affecting the levels. *Environ Res* **109**: 629-633.

Hiroi T, Okada K, Imaoka S, Osada M and Funae Y (2006) Bisphenol A binds to protein disulfide isomerase and inhibits its enzymatic and hormone-binding activities. *Endocrinology* **147**: 2773-2780.

Jiang C, Poole-Wilson PA, Sarrel PM, Mochizuki S, Collins P and MacLeod KT (1992) Effect of 17β-oestradiol on contraction, Ca^{2+} current and intracellular free Ca^{2+} in guinea-pig isolated cardiac myocytes. *Br J Pharmacol* **106**: 739-745.

Lang I, Galloway T, Scarlett A, Henley W, Depledge M, Wallace R and Melzer D (2011) Association of urinary bisphenol A concentration with medical disorders and laboratory abnormalities in adults. *JAMA* **300**: 1303-1310.

Linz KW and Meyer R (2000) Profile and kinetics of L-type calcium current during the cardiac ventricular action potential compared in guinea-pigs, rats and rabbits. *Pflugers Arch* **439**: 588-599.

Downloaded from molpharm.aspetjournals.org at ASPET Journals on April 17, 2024

Molecular Pharmacology Fast Forward. Published on November 29, 2012 as DOI: 10.1124/mol.112.081372
This article has not been copyedited and formatted. The final version may differ from this version.

Loganathan SN and Kannan K (2011) Occurrence of bisphenol A in indoor dust from two locations in the eastern United States and implications for human exposures. *Arch Environ Contam Toxicol* **61**: 68-73.

Matsushima A, Kakuta Y, Teramoto T, Koshiba T, Liu X, Okada H, Tokunaga T, Kawabata S, Kimura M and Shimohigashi Y (2007) Structural evidence for endocrine disruptor bisphenol A binding to human nuclear receptor ERRγ. *J Biochem* **142**: 517-524.

Matsushima A, Teramoto T, Okada H, Liu X, Tokunaga T, Kakuta Y and Shimohigashi Y (2008) ERR-γ tethers strongly bisphenol A and 4-α-cumylphenol in an induced-fit manner. *Biochem Biophys Res Commun* **373**: 408-413.

Melzer D, Rice NE, Lewis C, Henley WE and Galloway TS (2010) Association of urinary bisphenol a concentration with heart disease: evidence from NHANES 2003/06. *PLoS One* **5**: e8673.

Meyer R, Linz KW, Surges R, Meinardus S, Vees J, Hoffmann A, Windholz O and Grohe C (1998) Rapid modulation of L-type calcium current by acutely applied oestrogens in isolated cardiac myocytes from human, guinea-pig and rat. *Exp Physiol* **83**: 305-321.

Nakajima A, Saigusa D, Tetsu N, Yamakuni T, Tomioka Y and Hishinuma T (2009) Neurobehavioral effects of tetrabromobisphenol A, a brominated flame retardant, in mice. *Toxicol Lett* **189**: 78-83.

Nakajima T, Kitazawa T, Hamada E, Hazama H, Omata M and Kurachi Y (1995) 17β-Estradiol inhibits the voltage-dependent L-type Ca^{2+} currents in aortic smooth muscle cells. *Eur J Pharmacol* **294**: 625-635.

O'Reilly AO, Eberhardt E, Weidner C, Alzheimer C, Wallace BA and Lampert A (2012) Bisphenol A binds to the local anesthetic receptor site to block the human cardiac sodium channel. *PLoS One* **7**: e41667.

Okada H, Tokunaga T, Liu X, Takayanagi S, Matsushima A and Shimohigashi Y (2008) Direct evidence revealing structural elements essential for the high binding ability of bisphenol A to human estrogen-related receptor-γ. *Environ Health Perspect* **116**: 32-38.

Pandey AK and Deshpande SB (2012) Bisphenol A depresses compound action potential of frog sciatic nerve in vitro involving Ca^{2+}-dependent mechanisms. *Neurosci Lett* **517**: 128-132.

Riu A, Grimaldi M, le Maire A, Bey G, Phillips K, Boulahtouf A, Perdu E, Zalko D, Bourguet W and Balaguer P (2011) Peroxisome proliferator-activated receptor γ is a target for halogenated analogs of bisphenol A. *Environ Health Perspect* **119**: 1227-1232.

Rubin BS (2011) Bisphenol A: an endocrine disruptor with widespread exposure and multiple effects. *J Steroid Biochem Mol Biol* **127**: 27-34.

Sathyanarayana S, Braun JM, Yolton K, Liddy S and Lanphear BP (2011) Case report: high prenatal bisphenol a exposure and infant neonatal neurobehavior. *Environ Health Perspect* **119**: 1170-1175.

Sochivko D, Pereverzev A, Smyth N, Gissel C, Schneider T and Beck H (2002) The $Ca_V2.3$ Ca^{2+} channel subunit contributes to R-type Ca^{2+} currents in murine hippocampal and neocortical neurones. *J Physiol* **3**: 699–710.

Soriano S, Alonso-Magdalena P, Garcia-Arevalo M, Novials A, Muhammed SJ, Salehi A, Gustafsson JA, Quesada I and Nadal A (2012) Rapid insulinotropic action of low doses of bisphenol-A on mouse and human islets of Langerhans: role of estrogen receptor β. *PLoS One* **7**: e31109.

Swedenborg E, Ruegg J, Makela S and Pongratz I (2009) Endocrine disruptive chemicals: mechanisms of action and involvement in metabolic disorders. *Mol Endocrinol* **43**: 1-10.

Taylor JA, vom Saal FS, Welshons WV, Drury B, Rottinghaus G, Hunt PA, Toutain P-L, Laffont CM and VandeVoort CA (2010) Similarity of bisphenol A pharmacokinetics in rhesus monkeys and mice: relevance for human exposure. *Environ Health Perspect* **119**: 422-430.

U.S.EPA (2010) Bisphenol A (CASRN 80-05-7). URL: http://www.epa.gov/iris/subst/0356.htm [accessed 16 October 2012], (Agency USEP ed) pp 1-22, Washington.

Vandenberg LN, Hauser R, Marcus M, Olea N and Welshons WV (2007) Human exposure to bisphenol A (BPA). *Reprod Toxicol* **24**: 139-177.

von Goetz N, Wormuth M, Scheringer M and Hungerbühler K (2010) Bisphenol A: how the most relevant exposure sources contribute to total consumer exposure. *Risk Anal* **30**: 473-487.

Downloaded from molpharm.aspetjournals.org at ASPET Journals on April 17, 2024

Molecular Pharmacology Fast Forward. Published on November 29, 2012 as DOI: 10.1124/mol.112.081372
This article has not been copyedited and formatted. The final version may differ from this version.

Wang F, Hua J, Chen M, Xia Y, Zhang Q, Zhao R, Zhou W, Zhang Z and Wang B (2012) High urinary bisphenol A concentrations in workers and possible laboratory abnormalities. *Occup Environ Med* **69**: 679-684.

Wang Q, Cao J, Zhu Q, Luan C, Chen X, Yi X, Ding H, Chen J, Cheng J and Xiao H (2011) Inhibition of voltage-gated sodium channels by bisphenol A in mouse dorsal root ganglion neurons. *Brain Res* **1378**: 1-8.

Welling A, Hofmann F and Wegener JW (2005) Inhibition of L-type Cav1.2 Ca^{2+} channels by 2,(4-morpholinyl)-8-phenyl-4H-1-benzopyran-4-one (LY294002) and 2-[1-(3-dimethyl-aminopropyl)-5- methoxyindol-3-yl]-3-(1H-indol-3-yl) maleimide (Gö6983). *Mol Pharmacol* **67**: 541-544.

Wolstenholme JT, Rissman EF and Connelly JJ (2011) The role of Bisphenol A in shaping the brain, epigenome and behavior. *Horm and Behav* **59**: 296-305.

Xu X-h, Zhang J, Wang Y-m, Ye Y-p and Luo Q-q (2010) Perinatal exposure to bisphenol-A impairs learning-memory by concomitant down-regulation of N-methyl-d-aspartate receptors of hippocampus in male offspring mice. *Horm Behav* **58**: 326-333.

Downloaded from molpharm.aspetjournals.org at ASPET Journals on April 17, 2024

Molecular Pharmacology Fast Forward. Published on November 29, 2012 as DOI: 10.1124/mol.112.081372
This article has not been copyedited and formatted. The final version may differ from this version.

Figure legends

Fig. 1: BPA inhibits high voltage-activated (HVA) whole-cell Ba^{2+} currents in GH_3 cells. **(A)** Concentration-dependent inhibition of Ba^{2+} (5 mM) currents by BPA. Currents were elicited by depolarizing steps (50 ms) to 0 mV at 0.1 Hz. Increasing concentrations of BPA (as indicated) were successively applied for 40 s. Note that the current recovered completely upon washout of 100 µM BPA. **(B)** Time-course of current inhibition by BPA (100 µM). Currents were evoked by brief depolarizing steps (15 ms) to 0 mV at 1 Hz. Current amplitudes were measured 10 ms after beginning of the depolarization and current inhibition (%) was plotted vs. time. Application of BPA is indicated by the vertical bar. (**C)** Charge-voltage-relationship (C/V) for total Ba^{2+} currents for control (circles) and in the presence of 70 µM BPA (squares; n = 3). Data points represent the charge transferred for each current pulse (100 ms). Solid lines represent fit of data points to the equation given in Materials and Methods. BPA did not significantly affect values for half maximum activation (m_∞; control: -10.3 ± 0.9 mV, BPA: -4.9 ± 2.7 mV; $p > 0.07$). Inset shows fractional block for the data from Fig. 1C. **(D1)** Summary of pharmacological dissection of HVA Ba^{2+} currents using ω-conotoxin GVIA (1.5 µM), ω-conotoxin MVIIC (1.5 µM), nifedipine (10 µM) or nifedipine plus ω-conotoxin MVIIC. Current inhibition of normalized peak currents is shown in percent (n as indicated in brackets). **(D2)** Contribution of the different Ca^{2+} channel types to the total Ba^{2+} current. **(E1)** Normalized peak current inhibition (%) of total Ba^{2+} current by BPA (70 µM). **(E2)** Inhibition of pharmacologically dissected Ba^{2+} current fractions by BPA (70 µM; n as indicated in brackets; drug concentrations as in D1). **(F)** Concentration-effect relationship (CER) for BPA-mediated inhibition of total (filled symbols) or P/Q- (+R-)-type HVA currents (open symbols). CERs were obtained by plotting normalized peak current inhibition (%) against BPA concentration. Data points were fitted to a logistic function

Downloaded from molpharm.aspetjournals.org at ASPET Journals on April 17, 2024

Molecular Pharmacology Fast Forward. Published on November 29, 2012 as DOI: 10.1124/mol.112.081372
This article has not been copyedited and formatted. The final version may differ from this version.

yielding an EC_{50} of 26 ± 1.1 and 32 ± 1.9 µM for total and P/Q- (+R-)-type HVA currents, respectively (n = 3-9; see Table 1).

Fig. 2: BPA inhibits L-, N- and T-type Ca^{2+} channels in different tissues with similar potency. (A1) Summary of pharmacological characterization of HVA Ca^{2+} channels in mouse DRG neurons. Inhibition (%) of normalized HVA Ba^{2+} currents by ω-Agatoxin-TK (0.2 µM), nifedipine (10 µM), and ω-conotoxin GVIA (0.5 µM) (n=3-5). **(A2)** Contribution of different Ca^{2+} channel types to the total Ba^{2+} current. Note that the majority of Ba^{2+} currents (78 ± 0.6%) is through N-type Ca^{2+} channels. **(B)** CER for BPA-mediated inhibition of HVA N- (+R) type and **(C)** LVA T-type in DRG neurons and **(D)** L-type HVA Ca^{2+} channels in cardiac myocytes. CERs were obtained by plotting normalized peak current inhibition (%) against BPA concentration. Values for EC_{50} and Hill slope were obtained by fitting the data points to a logistic function. EC_{50} values for N-, T-and L-type channels were 35 ± 1.3 µM, 26 ± 1.2 µM and 35 ± 1.3 µM, respectively (n = 3- 8; see Table 1). For isolation of HVA and LVA Ca^{2+} channels in DRG neurons see Methods.

Fig. 3: BPA inhibits R-type Ca^{2+} channels expressed in HEK293 cells. (A) Ba^{2+} (15 mM) currents elicited by depolarizing steps (100 ms) to the potentials indicated are shown for control (left panel), in the presence of BPA (35 µM; middle panel), and upon washout (right panel). **(B)** Charge-voltage-relationship (C/V) for total Ba^{2+} currents. Data points represent the charge transferred by current pulses at different depolarizing voltages for control (n = 4; circles) and in the presence of 35 µM BPA (n = 4; squares), respectively. **(C)** CER for inhibition of Ba^{2+} currents by BPA is not dependent on resting-membrane potential. Currents were evoked from a membrane potential of either -70 mV (filled circles) or -100 mV

Downloaded from molpharm.aspetjournals.org at ASPET Journals on April 17, 2024

Molecular Pharmacology Fast Forward. Published on November 29, 2012 as DOI: 10.1124/mol.112.081372
This article has not been copyedited and formatted. The final version may differ from this version.

(open circles). Normalized peak current inhibition (%) was plotted against BPA concentration and data points were fitted to a logistic function (at -70 mV: EC_{50} 26 ± 1.04 µM; Hill slope = 1.19 ± 0.06; at -100 mV: EC_{50} 32 ± 1.03 µM; Hill slope = 1.16 ± 0.06; n = 3-9).

Fig. 4: Effect of BPA on steady-state and gating properties of R-type Ca^{2+}channels in HEK293 cells (A) Voltage-dependence of activation (m_∞) and steady state inactivation (h_∞) are not affected by BPA (control: circles; BPA: squares). To determine activation curves membrane potential was stepped for 1 s from -70 mV to -100 mV followed by depolarizing steps (10 ms) to potentials between -100 mV and +70 mV. Tail currents were recorded on repolarization to -70 mV. Normalized tail current amplitudes were plotted versus test potential. Steady-state inactivation was expressed as the ratio of two test pulses to +20 mV, separated by a 2 s inactivating pulse to membrane potentials between -100 and +5 mV. Normalized peak current amplitudes were plotted against membrane potential and data points were fitted to a Boltzmann function (m_∞: $V_{0.5}$ = 5.0 ± 1.1 mV; k = 12.5 and $V_{0.5}$ = 5.7 ± 1.0 mV; k = 11.3 (n = 6); h_∞: $V_{0.5}$ -73 ± 1.8 mV; k = 11.6 and $V_{0.5}$ -72.8 ± 1.2 mV; k = 12.1; (n = 4) for control and 35 µM BPA, respectively). **(B)** The time course for recovery from inactivation was obtained using a double pulse protocol (see inset) and is plotted as the ratio of peak current amplitudes (%) against the interpulse interval. Recovery from inactivation was not significantly different in the presence of BPA (35 µM; p = 0.824; n = 4-9). **(C)** BPA (70 µM) does not influence tail current kinetics. Tail currents were measured on repolarization to -80 mV following depolarizing steps (10 ms) from -50 mV to +80 mV in the presence or absence BPA. Inset: Normalized tail currents of Fig. 4C show similar current decay kinetics. The tail current decay could be fitted to a single exponential function with a time constant (τ) of 366 ± 30 µs (control) and 383 ± 33 µs (BPA), respectively (fit range is indicated by vertical lines; p = 0.73; n = 3).

Downloaded from molpharm.aspetjournals.org at ASPET Journals on April 17, 2024

Molecular Pharmacology Fast Forward. Published on November 29, 2012 as DOI: 10.1124/mol.112.081372
This article has not been copyedited and formatted. The final version may differ from this version.

Fig. 5: BPA´s action requires binding to the resting state of the R-type Ca^{2+}channel. When BPA (70 µM) was applied before the onset of a depolarizing step (100 ms) to 0 mV (pre-application) its effectiveness increased with pre-application time. **(A)** Bars represent normalized peak current amplitude inhibition (%) after different pre-application times. After 10 s inhibition was almost complete and did not increase significantly with longer pre-application times ($p > 0.05$ for 10 s vs. 20 s and 10 s vs. 40 s, n = 3-4). **(B)** BPA was completely ineffective when applied after the onset of the depolarizing step. Representative current traces shown for control and coapplication of BPA. Application time is indicated by the vertical bar. **(C)** Current traces were elicited by 1 s depolarizing steps to -10 mV and were recorded before (control) and three minutes after incubation with BPA (35 µM). No channel openings were elicited during the incubation period. Note that the block by BPA was fully developed after incubation and that Ca^{2+} channel kinetics were not altered. Current decay was fitted to a double exponential function. The time constants for control and BPA were τ_1: 63 ± 9 ms and 43 ± 3.6 ms, τ_2: 299 ± 58 ms and 261 ± 41 ms, respectively (τ_1: $p = 0.8$; τ_2: $p = 0.6$, n = 5). **(D)** Normalized traces from Fig. C.

Fig. 6: BPA´s action is independent of intracellular signaling pathways on R-type Ca^{2+} channels in HEK293 cells. The modulators of intracellular signaling pathways GTP-γ-S (20 µM), GDP-β-S (1 mM) (G-proteins), GÖ-6983 (10 µM) (PKC inhibitor) and H-89 (10 µM) (PKA inhibitor) had no effect on BPA (70 µM; control) induced Ba^{2+} current inhibition. G-protein modulators were added to the internal solution and allowed for 10 min to diffuse into the cell before current recording started. PKC and PKA inhibitors were applied via bath for up to 10 min. Currents were elicited by voltage ramps ranging from -70 mV to +50 mV for 50 ms every 15 s. ($p > 0.35$; n = 3-10)

Downloaded from molpharm.aspetjournals.org at ASPET Journals on April 17, 2024

Molecular Pharmacology Fast Forward. Published on November 29, 2012 as DOI: 10.1124/mol.112.081372
This article has not been copyedited and formatted. The final version may differ from this version.

Fig. 7: **BPA and 17β-estradiol (E_2) interact with different binding sites at the R-type Ca^{2+} channels in HEK293 cells. (A)** Time course of current inhibition by BPA (100 µM), E_2 (100 µM) and BPA + E_2 (100 µM each). Vertical bars indicate application period of the drugs. Ba^{2+} currents were evoked by voltage ramps (100 ms) from -70 mV to +50 mV at 0.1 Hz. **(B)** Average inhibition of Ba^{2+} currents by E_2, BPA or both at the concentrations indicated (µM). Inhibition of mean peak current in (%) was E_2 (30 µM): 19.1 ± 1.5 % n = 4; E_2 (100 µM): 40.7 ± 2.3 %, n = 14; E_2 (200 µM): 51.8 ± 2.7 %, n = 4. Significant differences are indicated above the columns (* $p < 0.05$ ***: $p < 0.001$; n = 4 - 15).

Fig. 8: Structural requirements of BPA for inhibition of HVA Ca^{2+} channels in GH_3 cells. Comparison of BPA to various bisphenolic **(A)** and phenolic **(B)** compounds. Ba^{2+} currents were elicited by applying voltage ramps (100 ms) from -70 mV to +50 mV. Compounds (100 µM) were applied 15 s before the onset of the voltage ramps and washed out immediately after return to the holding potential. Onset of the block was fast and recovery was complete for all compounds applied except for BPM and BPP. Bars illustrate normalized peak current amplitude reduction (%) induced by the various compounds (systematic names for compounds and statistical values are given in Table 2).

Downloaded from molpharm.aspetjournals.org at ASPET Journals on April 17, 2024

Molecular Pharmacology Fast Forward. Published on November 29, 2012 as DOI: 10.1124/mol.112.081372
This article has not been copyedited and formatted. The final version may differ from this version.

Tabel 1: Summary of the EC_{50} values of CERs*

tissue	Ca^{2+} channel	EC_{50} ± SEM§	Hill slope
GH_3 cells	total currents	26 ± 1.12	1.05
GH_3 cells	P/Q- (+ R-) type	32 ± 1.9	1.18
Cardiac myocytes	L- type	35 ± 1.3	1.39
DRG neurons	N- (+ R-) type	35 ± 1.3	1.12
DRG neurons	T- type	26 ± 1.12	0.84
HEK cells (HP# -70 mV)	R- type $Ca_V2.3$	26 ± 1.04	1.19
HEK cells (HP# -100 mV)	R- type $Ca_V2.3$	32 ± 1.03	1.16

*Concentration-effect relationship
#Holding potential §(p = 0.97 for all CERs; n = 3-8 for each concentration)

Downloaded from molpharm.aspetjournals.org at ASPET Journals on April 17, 2024

Molecular Pharmacology Fast Forward. Published on November 29, 2012 as DOI: 10.1124/mol.112.081372
This article has not been copyedited and formatted. The final version may differ from this version.

Table 2: Effect of various phenolic and bisphenolic compounds on HVA Ba^{2+} currents in GH_3 cells in relation to BPA.

Systematic Name	Abbreviation	Inhibition % ± SEM	Significance[§]
2,2-bis(4-hydroxyphenyl)propane	BPA	83 ± 2.1	
4-(1-methyl-1-phenylethyl)-phenol	4´-CP	45 ± 4.5	***
1,1'-(1-methylethylidene)bis-benzene	2,2´-DPP	17 ± 2.8	***
4,4'-(1,1,1,3,3,3-hexafluoro-2,2-propanediyl)diphenol	BPAF	100 ± 0	***
4,4'-ethylidene-diphenol	BPE	57 ± 2.8	***
4,4'-(2,2-butanediyl)diphenol	BPAB	83 ± 2.1	–
4,4'-methylenebis-phenol	BPF	30 ± 2.4	***
4,4'-dihydroxybenzophenone	4,4´-HBP	19 ± 2.5	***
4,4'-sulfonyldiphenol	BPS	13 ± 1.7	***
4'-diol-1,1-biphenyl	Biphenol	20 ± 1.7	***
4,4'-(1-methylethylidene)bis-2,6-dibromo-phenol	TBBA	72 ± 2.5	**
4,4'-isopropylidenebis(2,6-dimethylphenol)	TMBPA	40 ± 1.5	***
4-tert-butyl-phenol	4´-TBP	27 ± 2.5	***
4-(1,1-dimethylpropyl)-phenol	4´-TAP	48 ± 2.3	***
4,4'-((p-phenylene)diisopropylidene)diphenol	BPM	66 ± 3.7	**
4,4'-((p-phenylene)diisopropylidene)diphenol	BPP	16 ± 2.0	***

Drug concentration 100µM

[§]Significant differences to BPA determined by ANOVA &Tukey´s test; **: $p \leq 0.01$; ***: $p \leq 0.001$; n = 3-10.

Downloaded from molpharm.aspetjournals.org at ASPET Journals on April 17, 2024

Figure 1

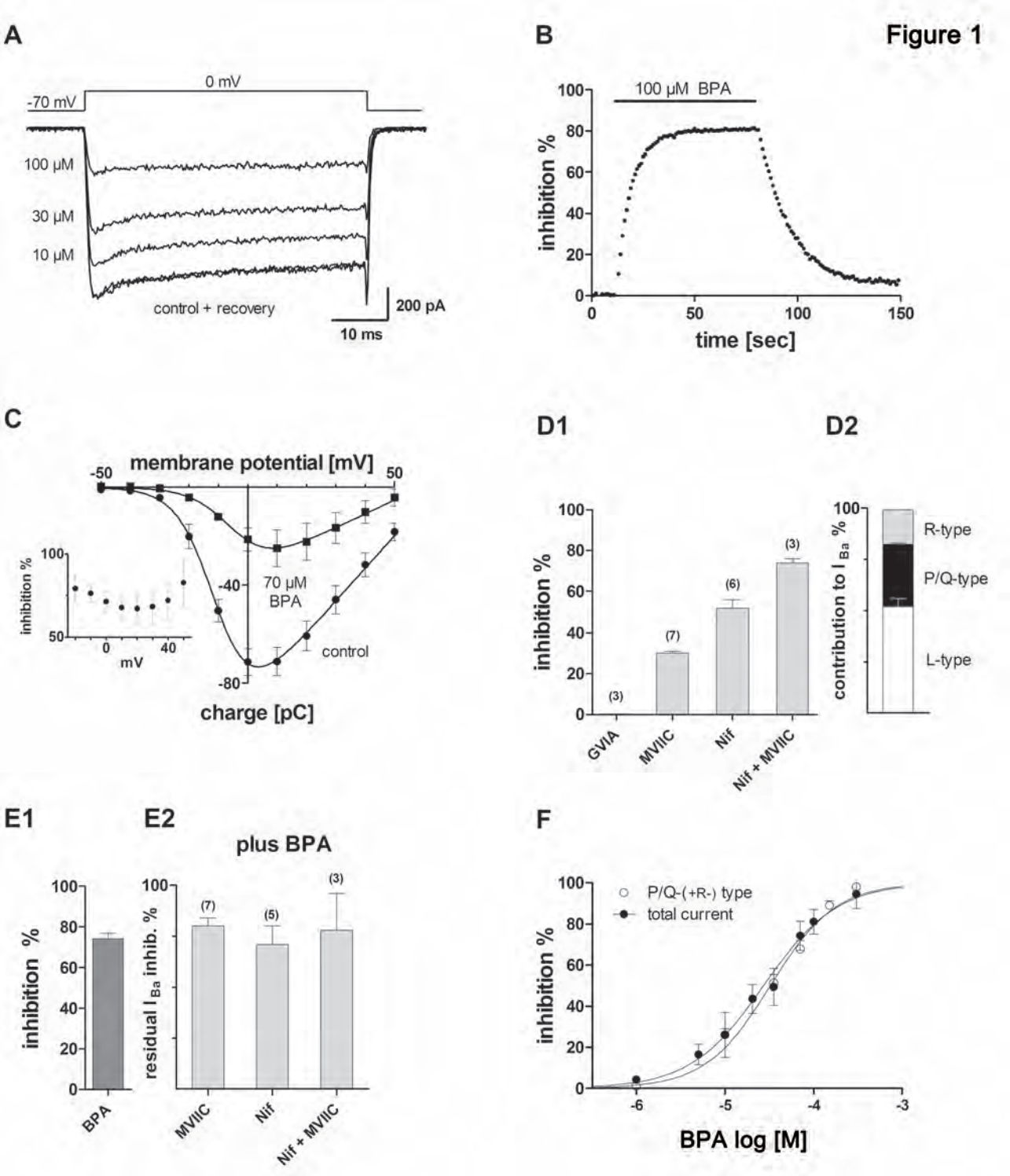
A
0 mV
-70 mV
100 µM
30 µM
10 µM
control + recovery
200 pA
10 ms
B
100 µM BPA
inhibition %
time [sec]
C
membrane potential [mV]
-50
50
-40
-80
70 µM BPA
control
inhibition %
mV
charge [pC]
D1
D2
inhibition %
(3)
(7)
(6)
(3)
GVIA
MVIIC
Nif
Nif + MVIIC
contribution to I Ba %
R-type
P/Q-type
L-type
E1
E2
plus BPA
inhibition %
residual I Ba inhib. %
BPA
MVIIC
Nif
Nif + MVIIC
F
P/Q-(+R-) type
total current
inhibition %
BPA log [M]

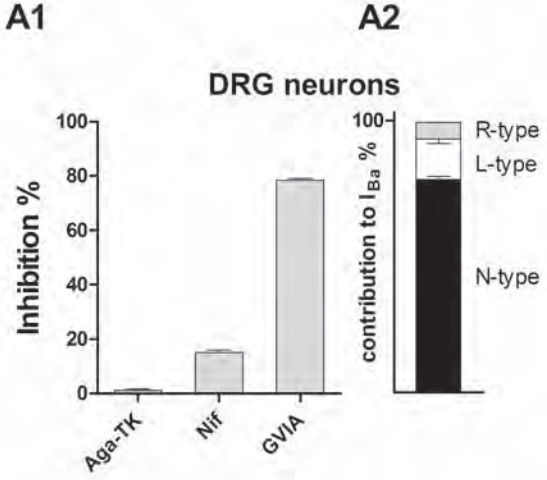
A1
A2
DRG neurons
Inhibition %
100
80
60
40
20
0
Aga-TK
Nif
GVIA
contribution to I_{Ba} %
R-type
L-type
N-type

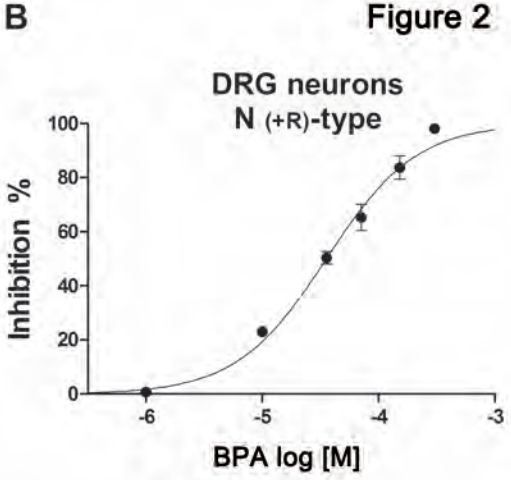
B
DRG neurons
N (+R)-type
Inhibition %
BPA log [M]
-6
-5
-4
-3

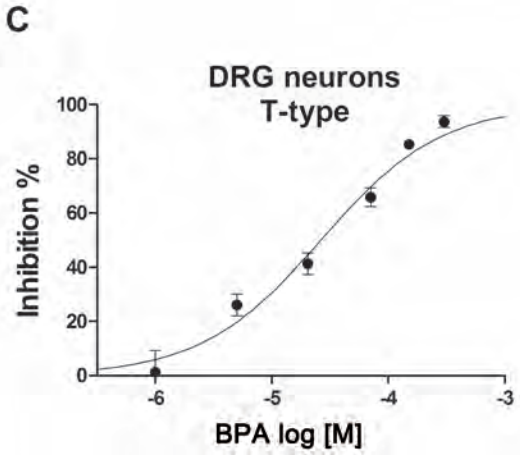
C
DRG neurons
T-type
Inhibition %
BPA log [M]

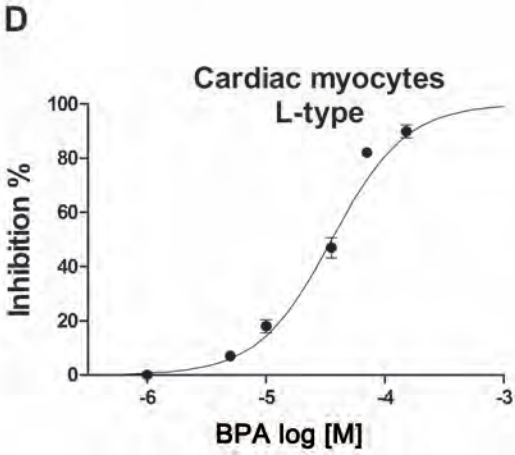
D
Cardiac myocytes
L-type
Inhibition %
BPA log [M]

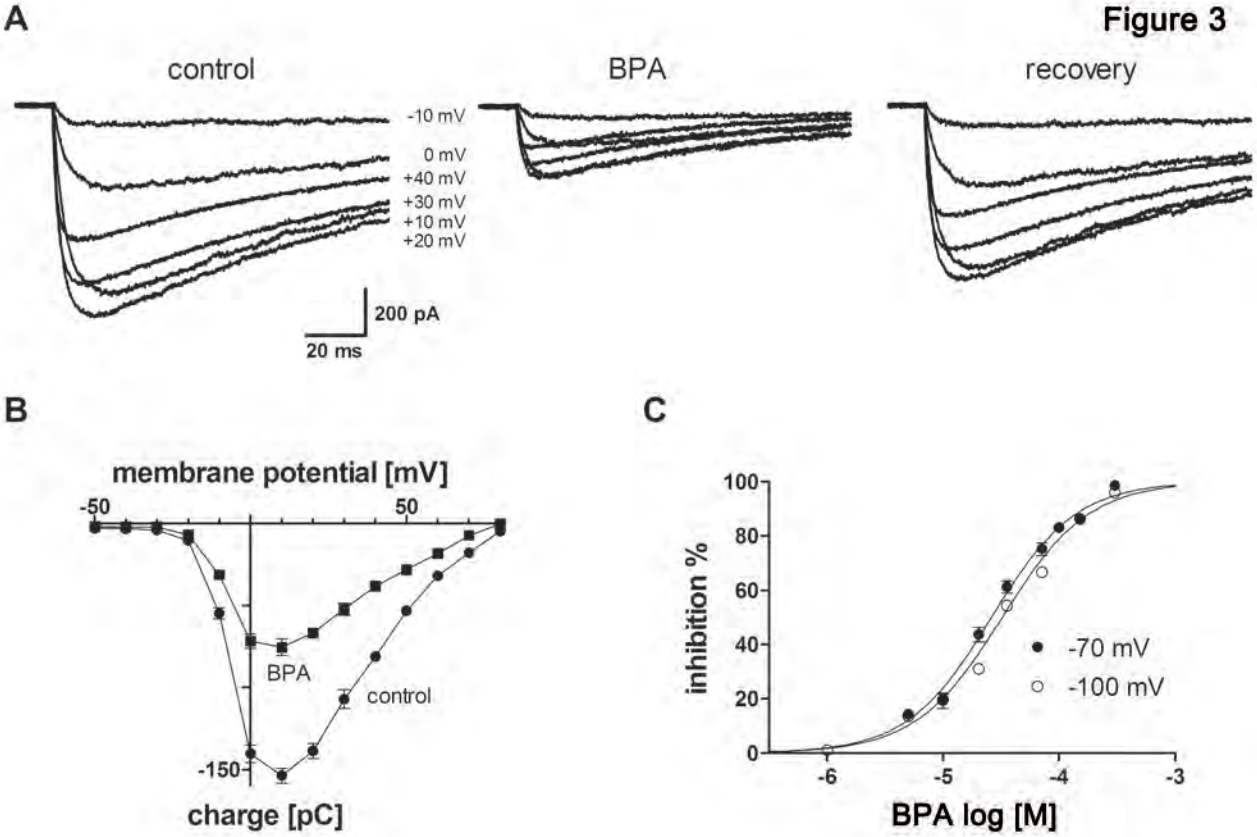
A
Figure 3
control
BPA
recovery
-10 mV
0 mV
+40 mV
+30 mV
+10 mV
+20 mV
200 pA
20 ms
B
membrane potential [mV]
-50
50
BPA
control
-150
charge [pC]
C
100
80
60
40
20
0
inhibition %
-70 mV
-100 mV
-6
-5
-4
-3
BPA log [M]

Figure 4

A

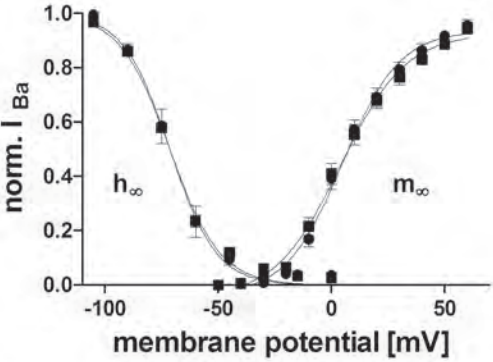
norm. I Ba
1.0
0.8
0.6
0.4
0.2
0.0
h∞
m∞
-100
-50
0
50
membrane potential [mV]

B

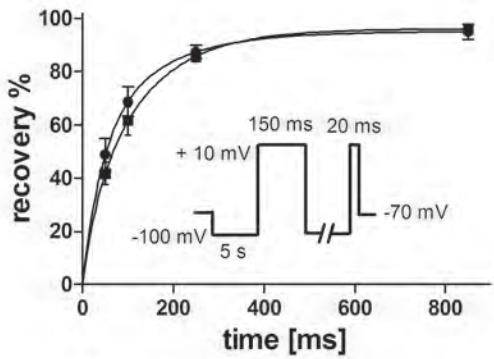
recovery %
100
80
60
40
20
0
150 ms
20 ms
+ 10 mV
-70 mV
-100 mV
5 s
0
200
400
600
800
time [ms]

C

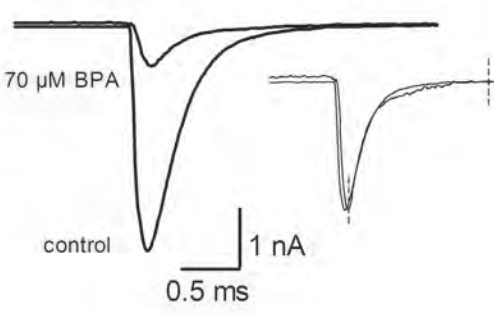
70 µM BPA
control
1 nA
0.5 ms

Figure 5

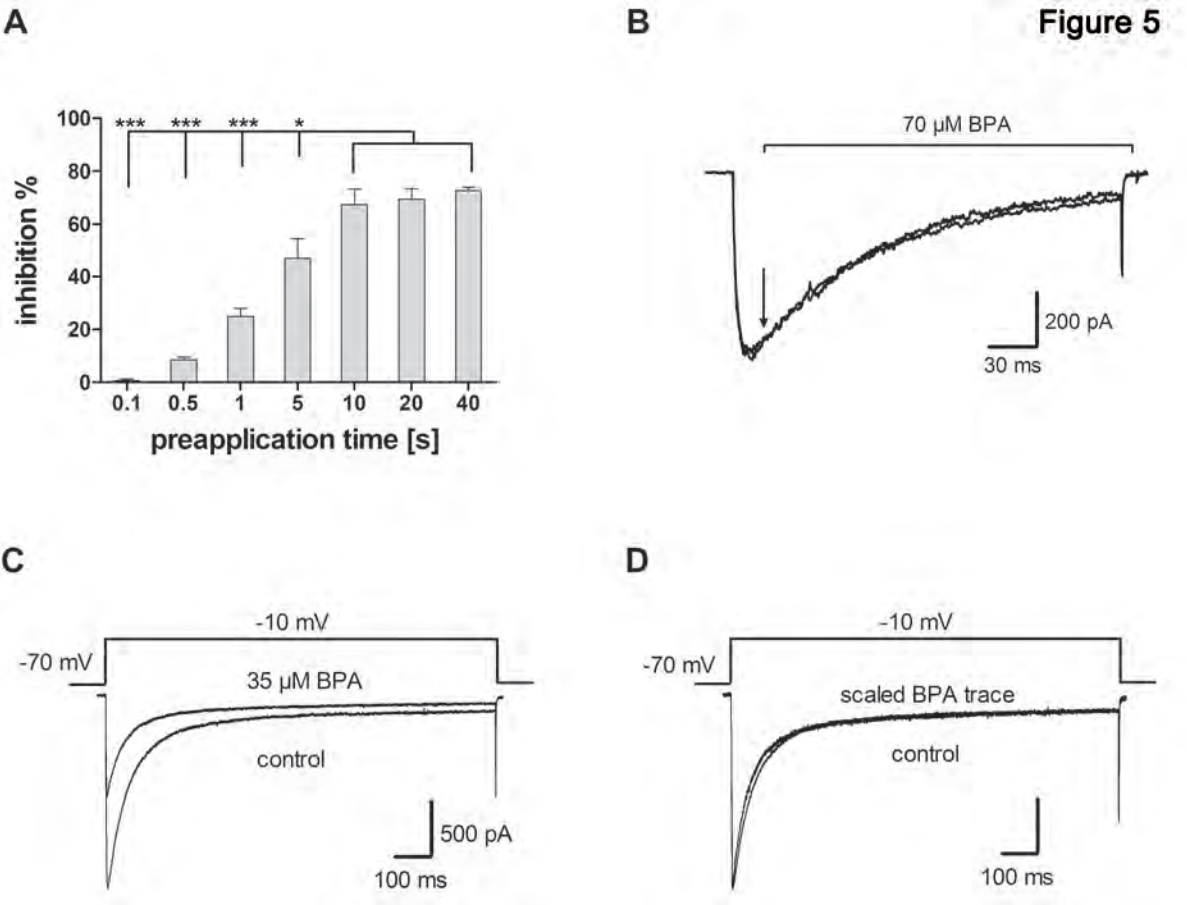
A
B
C
D
inhibition %
100
80
60
40
20
0
***
***
***
*
0.1
0.5
1
5
10
20
40
preapplication time [s]
70 µM BPA
200 pA
30 ms
-10 mV
-70 mV
35 µM BPA
control
500 pA
100 ms
-10 mV
-70 mV
scaled BPA trace
control
100 ms

Figure 6

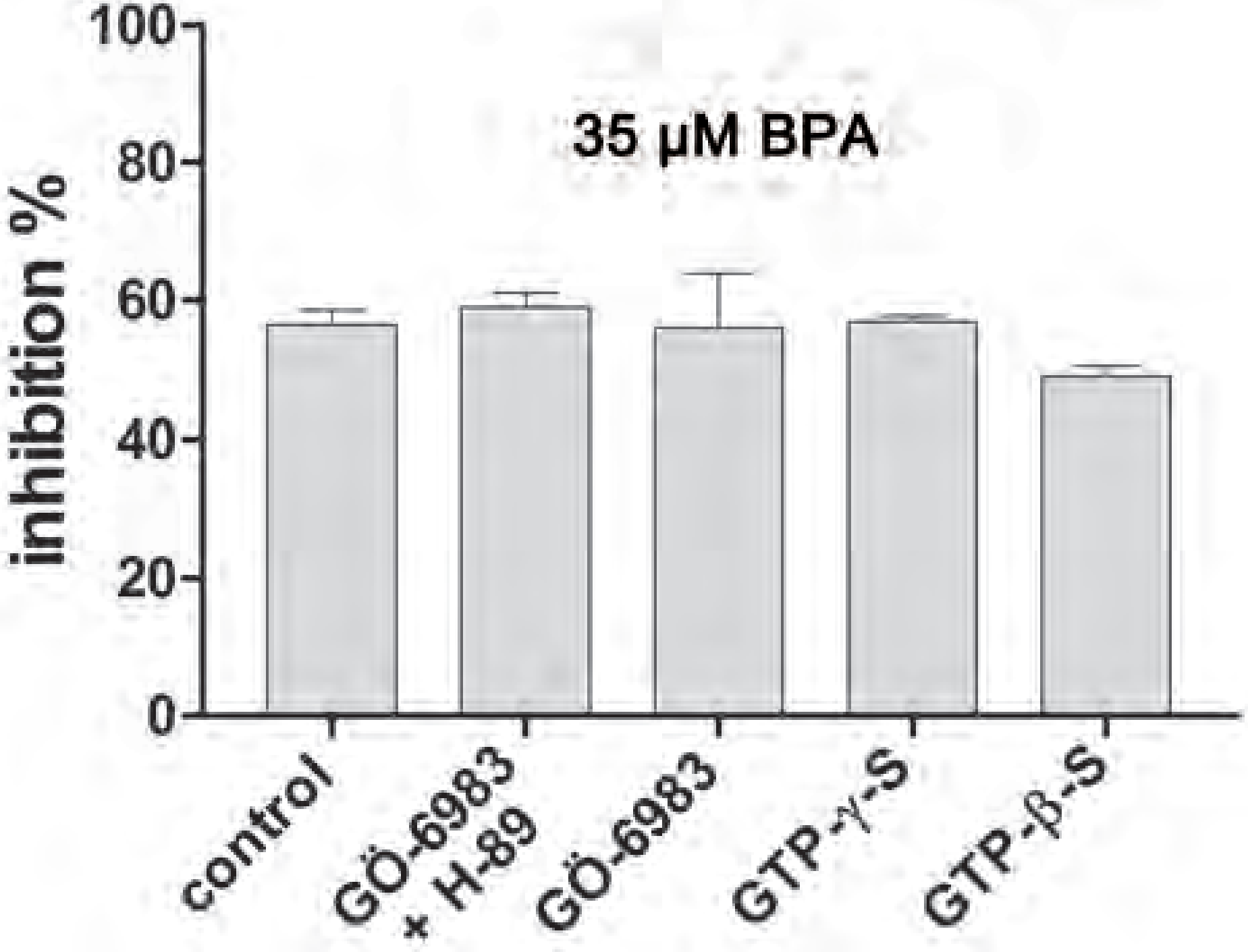
35 µM BPA
inhibition %
100
80
60
40
20
0
control
GÖ-6983 + H-89
GÖ-6983
GTP-γ-S
GTP-β-S

Figure 7

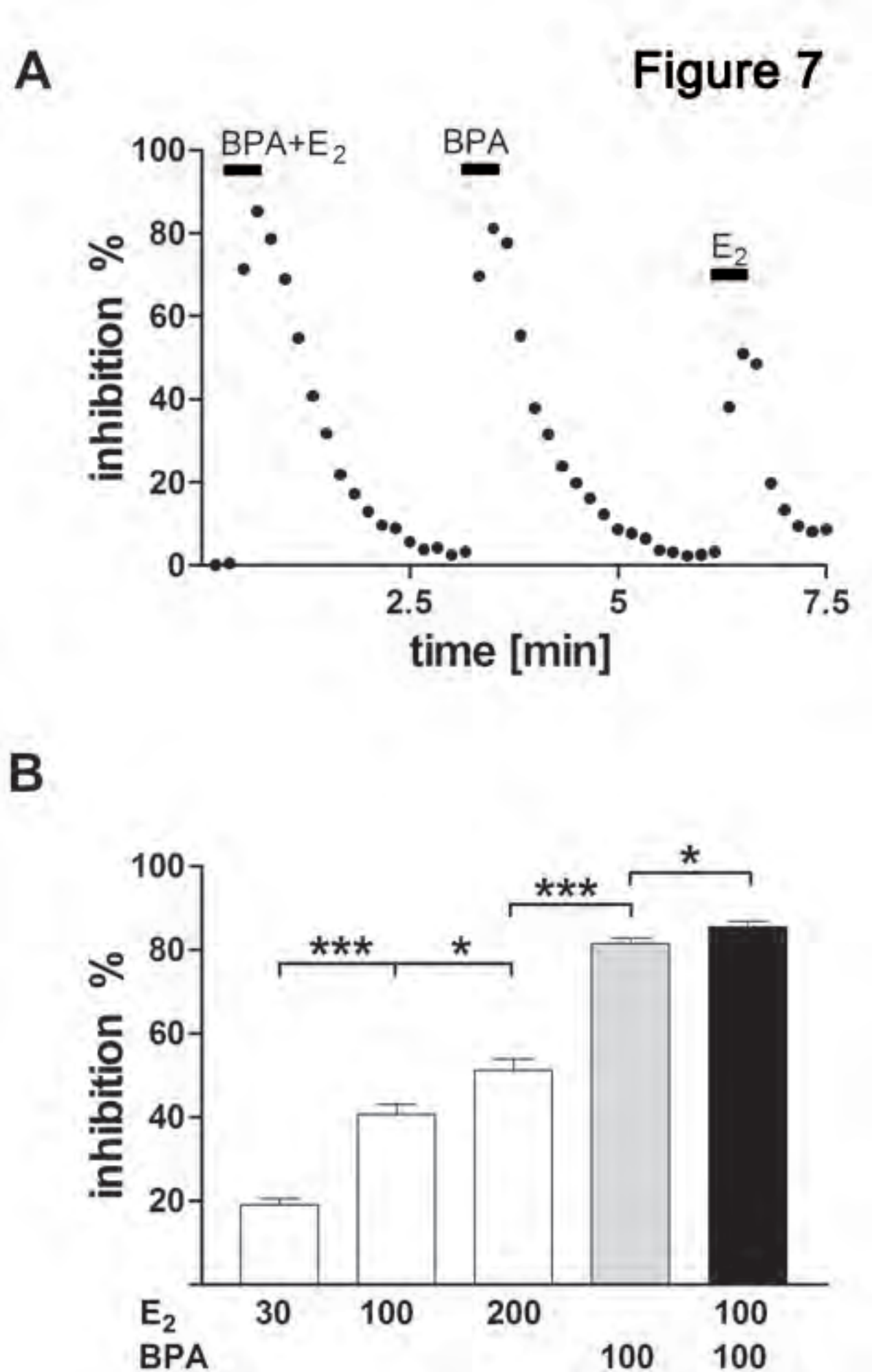
A
BPA+E2
BPA
E2
100
80
60
40
20
0
inhibition %
2.5
5
7.5
time [min]
B
100
80
60
40
20
inhibition %
***
*
***
*
E2
30
100
200
100
BPA
100
100

Figure 8

A

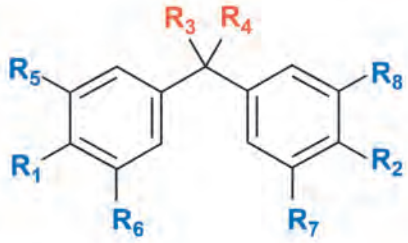
R3
R4
R5
R8
R1
R2
R6
R7

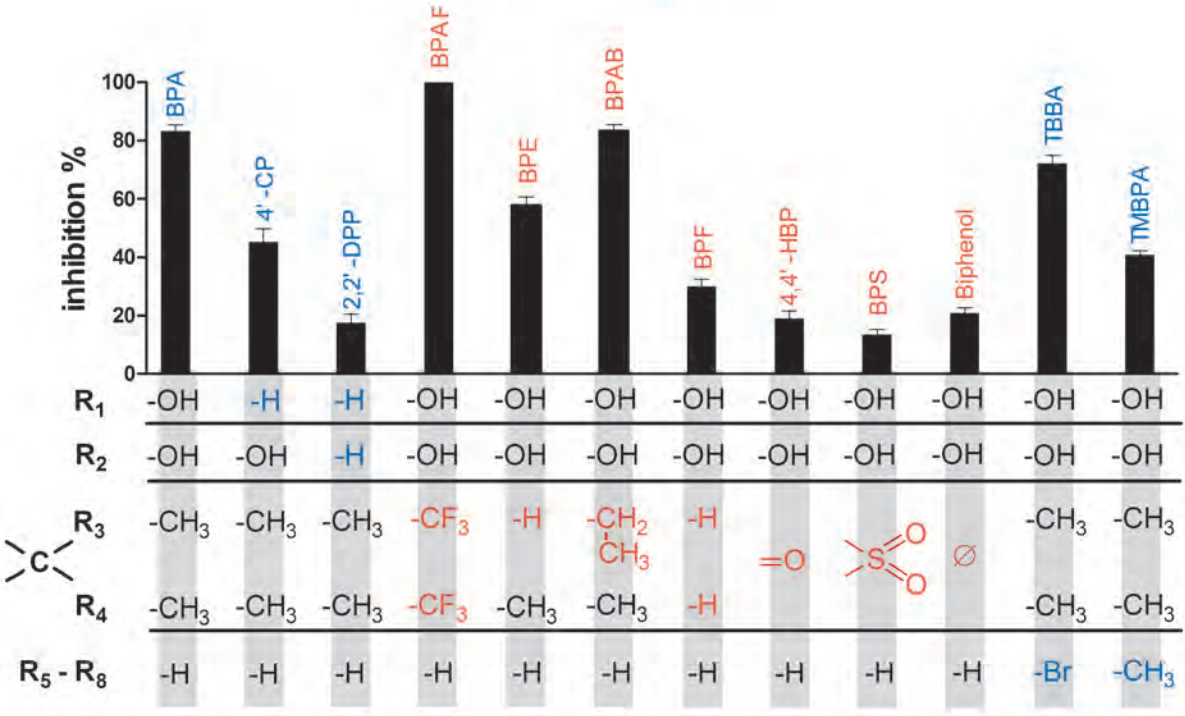
inhibition %
100
80
60
40
20
0
BPA
4'-CP
2,2'-DPP
BPAF
BPE
BPAB
BPF
4,4'-HBP
BPS
Biphenol
TBBA
TMBPA
R1 -OH -H -H -OH -OH -OH -OH -OH -OH -OH -OH -OH
R2 -OH -OH -H -OH -OH -OH -OH -OH -OH -OH -OH -OH
R3 -CH3 -CH3 -CH3 -CF3 -H -CH2CH3 -H =O S(=O)2 ∅ -CH3 -CH3
R4 -CH3 -CH3 -CH3 -CF3 -CH3 -CH3 -H -CH3 -CH3
R5 - R8 -H -H -H -H -H -H -H -H -H -H -Br -CH3

B

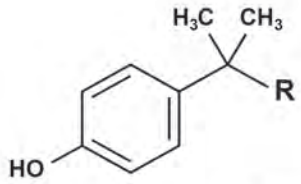
H3C CH3
R
HO

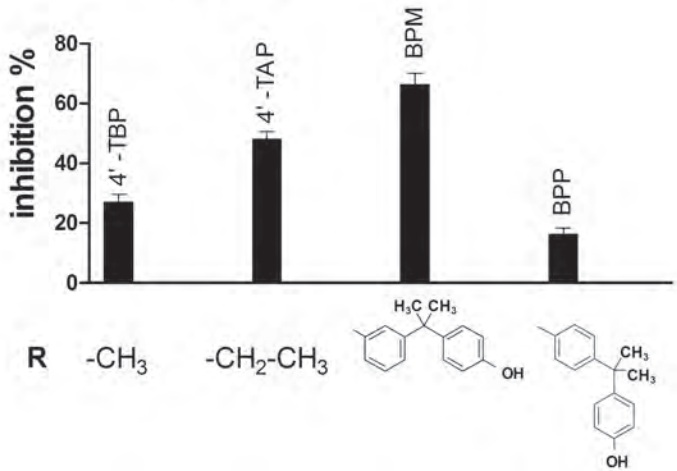
inhibition %
80
60
40
20
0
4'-TBP
4'-TAP
BPM
BPP
R -CH3 -CH2-CH3
H3C CH3
OH
CH3
CH3
OH